Desalination and Water Treatment
www.deswater.com

doi: 10.1080/19443994.2015.1077749

57 (2016) 16424–16434
July

Taylor & Francis
Taylor & Francis Group

A continuous-flow device for photocatalytic degradation and full mineralization of priority pollutants in water

Giora Rytwo[a,b,*], Tomer Klein[a,b], Sivan Margalit[a,b], Omer Mor[a], Aviv Naftali[a,b], Gonen Daskal[a]

[a]*Environmental Physical Chemistry Laboratory, MIGAL, Galilee Research Institute, Upper Galilee, Israel, Tel. +972 4 6953553; Fax: +972 4 6944980; emails: rytwo@telhai.ac.il (G. Rytwo), tomerklein15@gmail.com (T. Klein), margalit.sivan@gmail.com (S. Margalit), omi.mor@gmail.com (O. Mor), aviv.naftaly@gmail.com (A. Naftali), gonen.d@equashield.com (G. Daskal)*
[b]*Department of Environmental Sciences, Tel Hai College, Upper Galilee, Israel*

Received 22 June 2015; Accepted 25 July 2015

ABSTRACT

The removal of hazardous pollutants which are harmful, even at very low concentrations, to human health and the environment is a challenging task. Standard techniques used to remove such pollutants from water often produce a polluted sludge that needs to be disposed of as hazardous waste. Photocatalytic degradation is an advanced oxidation process that might allow full mineralization of the pollutant with zero discharge of hazardous waste. However, most current devices performing photocatalytic degradation processes usually suffer from low efficiency due to technical problems that hinder efficient contact between the pollutant, the light and the catalyst. The system presented in this study aims to optimize this contact and allows photodegradation of polluted effluent flowing continuously through it. The system was used to study photodegradation of acetaminophen and picric acid. Under UVC radiation (254 nm), both pollutants underwent non-catalyzed photodegradation that followed zero-order kinetics. However, the addition of TiO_2 accelerated the process, reducing half lives to 25% of their respective non-catalyzed values, and completely changing the reaction mechanism: the catalyzed processes obeyed second-order kinetics law. When a relatively low concentration (2 ppm) of pollutant was treated with the device, it was completely removed within about 1 h of irradiation time.

Keywords: Acetaminophen; Paracetamol; Picric acid; Photodegradation; Titanium dioxide; Catalysis; Advanced oxidation process

1. Introduction

Hazardous materials and pollutants removal from water is a growing environmental problem. Standard removal techniques create a polluted sludge that needs to be disposed of as hazardous waste. Catalytic degradation processes may allow full mineralization of the pollutant with zero discharge of hazardous waste. Advanced oxidation processes (AOPs) have proven to be among the most effective methods for water treatment [1]. In general, AOPs are based on the in situ generation of highly reactive transitory species (i.e. H_2O_2, $OH^{\bullet}$, $O_2^{-\bullet}$, O_3, etc.) that mineralize refractory organic compounds and other pollutants [2]. Among the AOPs, heterogeneous photocatalysis

*Corresponding author.

has demonstrated its efficiency in degrading a wide range of refractory organics into biodegradable compounds, and in some cases even yields complete mineralization to carbon dioxide and water. The large number of studies on that issue have been widely reported and reviewed in the scientific literature [3–6].

The most widely applied photocatalyst in water-treatment research is known as "Degussa P25" titanium dioxide (TiO_2), which consists of 80% anatase and 20% rutile with a surface area of 50 $m^2 g^{-1}$ [5,7]. This photocatalyst is generally assumed to exhibit a synergistic effect: the anatase phase has a large surface area, allowing contact with pollutants that are present at low concentrations; on the other hand, the relatively large rutile particles contribute more efficiently to the band-bending effect in water-molecule oxidation ("splitting water"), which is an essential part of the photocatalytic process [8]. However, this assumption has never been proven, and some studies have shown the same level of activity for separate TiO_2 phases and P25 [9]. Combinations of metal oxides or semiconductors (ZnO, Fe_2O_3, Fe_3O_4, CdS, GaP and ZnS), clay minerals [10–14], zeolites [15], pillared clays [16] and even pillared clays based on TiO_2 pillars [17,18] have also been used as photocatalysts.

The efficiency of photocatalysis is usually explained by a series of oxidative–reductive chain reactions that occur at the photon-activated surface. For TiO_2, photon energy ($h\nu$) should be greater than or equal to the bandgap energy of TiO_2 (usually 3.2 eV for anatase or 3.0 eV for rutile), causing the lone electron to be photoexcited to the empty conduction band in femtoseconds, followed by a series of processes [19] yielding efficient photocatalysis.

Heterogeneous photocatalytic processes can be separated into five independent steps [20]: (i) transfer of the reactants in the fluid phase to the surface, (ii) adsorption of a least one of these reactants, (iii) reaction in the adsorbed phase, (iv) desorption of the product(s), (v) removal of the products from the interface region. Given stages (i) and (v) can be easily controlled, the importance of the contact between the compounds and the catalysts (stages (ii)–(iv)) becomes evident: to induce a faster process, such contact should be enhanced as must as possible. This can be done by dispersing the catalyst on a vast volume of polluted effluent. However, crucial to this process is the occurrence of photon absorption while the pollutant is adsorbed on the catalyst. Thus, to increase the rate of the process, light must be supplied to this vast volume of effluent + catalyst. The main objective of this study was to develop a device that might enhance photocatalytic degradation of pollutants by allowing broad contact between catalyst, pollutant, and photons.

Photocatalytic reactors for water treatment are classified into two main configurations: (i) reactors with suspended photocatalyst particles ("slurry type") and (ii) reactors with photocatalyst immobilized onto an inert carrier [21]. The second configuration allows a relatively simpler continuous operation, whereas the first configuration requires an additional separation unit for the recovery of photocatalyst particles. Considering that the limiting factor for such a reactor is the contact between effluent, catalyst and light, a slurry-type photocatalytic reactor might yield higher rates. The problem is the separation of the photocatalyst particles. One setup involves settling tanks. However, such devices require coagulants and flocculants.

A technically promising solution is the application of hybrid photocatalytic/membrane processes [3]. These reactors are based on immobilized catalysts, and the photocatalysis occurs on the membrane surface or in its pores [22]. Meng et al. [23] were the first to attempt to combine membrane and photocatalytic technologies. In continuous operation, intermittent backwash was used to retard membrane fouling. One of the main foulants on the membrane surface was the catalyst itself. Sequential rinsing using tap water and sodium hypochlorite was required to partly recover the permeability of the membrane. The authors concluded that even though the device can be used to treat polluted river water, a complete economic analysis is necessary to determine the method's economic viability.

An additional suggested setup to obtain the advantages of a photocatalytic slurry on the one hand, while allowing efficient slurry separation on the other, is "membrane distillation", which is a process of evaporating volatile feed components through a porous hydrophobic membrane [24]. Even though authors concluded that this is a very promising method [25], the process has not been applied commercially.

A setup that has matured to commercial application is the Photo-Cat™ apparatus (manufactured by Purifics Inc., London, Ontario, Canada). In that system, the water stream passes through a pre-filter bag and a cartridge filter before being mixed with a TiO_2 nanoparticle slurry stream. The mixed stream then passes through the reactor with UV lamps series. A TiO_2 recovery is hybridized downstream of the reactor to remove the catalyst allowing the treated water to exit. The TiO_2 stream is recycled and remixed with the fresh TiO_2 slurry stream entering the reactor [3]. To prevent fouling, the TiO_2 recovery unit is backpulsed with air for 0.5 s every 60 s.

This device was tested for the removal of 32 pollutants from water [7]. The authors found over

70% removal of 29 targeted compounds and estrogenic activity, while removal of the other 3 compounds was less than 50%. The study exhibited similar efficiencies in photocatalytic reactor membrane mode and photolytic mode. The authors could not explain why the catalyst did not improve the process, but speculated that it might be due to the relatively low catalyst concentration (50 ppm), the relatively fast passage through the device, or both.

Herein we present an efficient and relatively low-cost device for the continuous photodegradation of organic hazardous compounds. Complete mineralization was observed in several cases. The device can be optimized for the pollutant by controlling several parameters, such as flow rate, auxiliary compounds (air, O_2, H_2O_2), type and concentration of catalyst in the slurry, and even photon energy by changing the lamp.

2. Materials and methods

2.1. Description of the device

In this study, a photochemical flow device was developed, which is fully described in [26]. The device consists of an inner tube with a UV lamp, and an outer tube in which the catalyst and the polluted effluents flow (Fig. 1(a) and (b)). The effluent is pumped into the outer cylinder from one of the inlets by the main pump (Fig. 1(b)). In the outer cylinder, the polluted effluent is mixed with catalyst slurry (P25 TiO_2, clay, pillared clay, or any other suitable material). While flowing in the outer tube, the mixture of polluted effluent and catalyst is irradiated by the UV lamp in the inner cylinder. The liquid in the outer cylinder is slightly stirred by the stirring rods (Fig. 1(a)) at low velocity, to avoid settling of the catalyst without creating turbulence in the liquid. The liquid flows upward toward a 0.6-μm pore polytetrafluoroethylene (PTFE) membrane that stops the catalyst particles, and is constantly cleaned by a system based on suction and a rotating brush. The suctioned catalyst slurry is returned from the outlet at the top of the device (Fig. 1(a)) to the second inlet at the bottom of it (Fig. 1(b)). Additional auxiliary inlets/outlets are placed along the outer cylinder to allow for additional features, such as the introduction of air or oxygen. Other possible options (although not tested in this study) are reduction/oxidation agents, H_2O_2, O_3, or other auxiliary materials to enhance photocatalysis. In the specific device used in this study, the inner cylinder was made from quartz glass to ensure full transparency in the UV range. The UV lamp had an energy input of 20 W and a light output of 6.4 W at a wavelength of 254 nm. Considering the dimensions of the inner and outer cylinders, the flow area is approximately 2,900 mm^2 (29 cm^2). The main pump is electronically controlled and can deliver flows of 2–20 $cm^3\ min^{-1}$. Thus, flow velocity ranges from 0.7 to 7 mm min^{-1}, which considering the effective length of the lamp, yields irradiation times of 9–0.9 h, respectively. Such wide range of irradiation periods provides large flexibility that might cover a wide range of pollutant concentrations. A scheme of the working procedure is shown in Fig. 2.

2.2. Preliminary batch experiments

The main purpose of these experiments was to screen a series of pollutants, in order to determine the cases in which the use of a catalyst would considerably improve the photodegradation that might occur anyway, when irradiating organic pollutants with UVC light (254 nm). A wide range of pollutants was divided into three groups: (i) dyes, (ii) pharmaceuticals, (iii) phenols and polyphenols. Several catalysts were tested, among them TiO_2, raw and Cu-exchanged SWy-2 montmorillonite, SHCa-1 hectorite, and Li-synthetic hectorite. In the "batch" experiments, the concentration of each pollutant ranged between 20 and 150 μM, adjusted to obtain a UV–vis (VIS) optical density (OD) of 1.2–1.5; catalyst was then added at 0.2 g l^{-1} (when used). Suspensions were irradiated for 2 h in a RMR-600 Rayonet mini photochemical chamber reactor equipped with four 8-W RMR-1849/253.7 nm lamps, and the UV–vis spectrum was measured using a diode array HP8452 spectrophotometer with a quartz cuvette that was transparent to the whole UV–vis range (200–800 nm). The relative degradation of each pollutant at the wavelength of maximum absorption (λ_{max}) was evaluated as the ratio of actual to initial concentration (C/C_0). All materials were used without further purification or preparation.

2.3. Flow experiments

Since TiO_2 exhibited the best overall performance, most of the experiments with the flow device described in Section 2.1 were performed with Degussa P25 TiO_2.

2.3.1. Closed-system experiments

The device outflow was pumped to a flow-through cuvette placed in the diode-array UV–vis spectrophotometer, and then directly back into the device as inflow. Concentrations were monitored by the

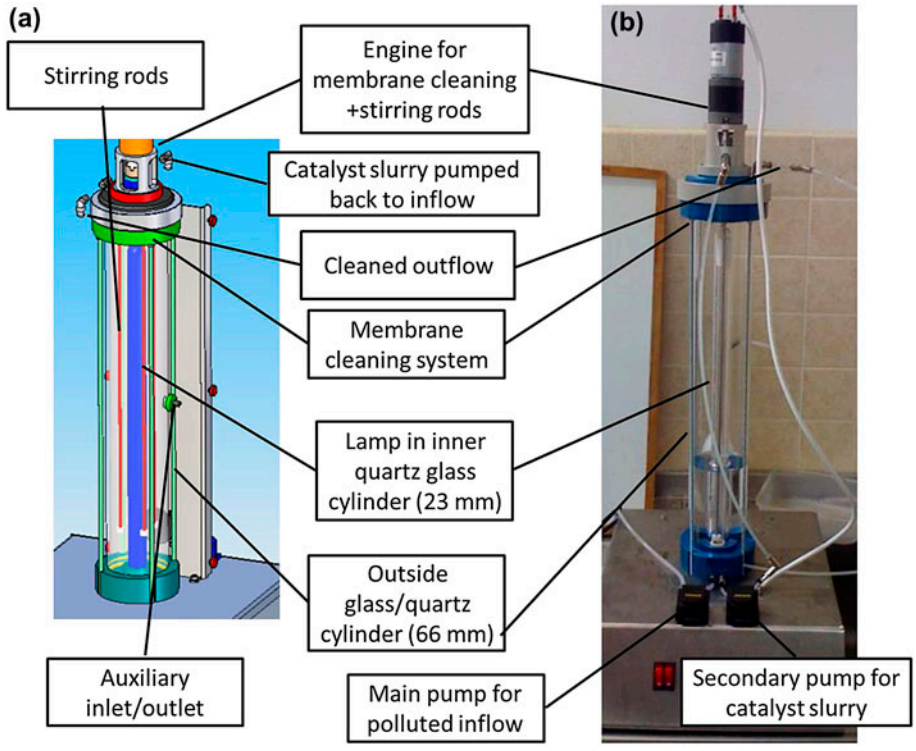

Fig. 1. General structure of the polluted effluent photodegradation system. (a) Schematic view and (b) photograph of an actual polluted effluent treatment system.

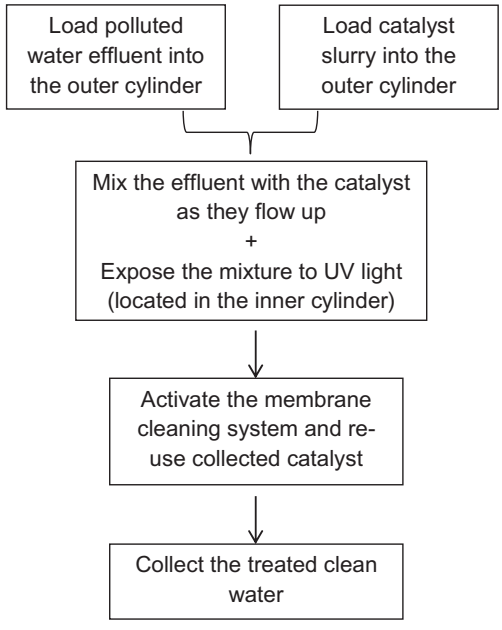

Fig. 2. Schematic diagram of the procedure performed by the photodegradation device.

"kinetics" module of Chemstation 06.03 software (Hewlett-Packard) on the HP8452A spectrophotometer. Kinetics analysis for fit to zero-, first- or second-order processes (see detailed explanation in Appendix 1) was performed on several wavelengths of the spectra. Experiments were performed for selected chemicals belonging to "dye", "phenol", and "pharmaceutical" groups.

2.3.2. Confirmation experiment

An additional a set of confirmatory experiments was performed on a few pollutants, in a closed system similar to that described in Section 2.3.1. Effluent was sampled at several time points, and concentration was measured by liquid chromatography mass spectrometry (LCMS) in an Agilent 6540 Q-TOF LCMS equipped with an Agilent 1290 UHPLC. LCMS measurements were performed with the ESI interface, and included screening for molecular weights lower than those of the original pollutant to monitor the presence of partially degraded compounds.

2.3.3. Open-system low-concentration experiments

Additional tests were performed to determine whether complete degradation of relatively low concentrations (2 ppm) of priority pollutants can be

achieved in one pass through the device (retention time of <2 h). Large volumes (5 l) of 2 ppm pollutant solution were prepared, the device was filled with the solution, and 0.1 g l^{-1} TiO_2 was added. An additional 3 l of effluent was connected to the device inflow. Measurements of the treated effluents at several time points after the start of the experiments were performed by LCMS with a limit of detection (LOD) of 1 ppb. The flow rate applied in the experiment was 18 ml min^{-1}, yielding an approximate irradiation time of 1.2 h. After 2.5 h, the lamp was shut off to monitor the increase in pollutant concentration due to lack of photocatalysis.

3. Results and discussion

3.1. Preliminary batch experiments

Table 1 shows the percentage of degradation of the tested pollutants, with or without catalyst, after 2 h of irradiation. Based on the preliminary experiments and in order to focus on the efficiency of the device, the following was considered for further experiments:

(1) Some of the tested compounds were considerably photodegraded when irradiated with UVC, even without catalyst. However, with all compounds tested, addition of catalyst yielded more photodegradation.

(2) Even though the preliminary results indicated that clay minerals may also act as catalysts, P25 TiO_2 was chosen for use in almost all of the experiments with the flow-through device.

3.2. Closed-system experiments

The closed-system flow experiments were performed with several of the chemical compounds presented in Table 1. For brevity, we report the results from two of these compounds: picric acid (PA; "phenols") and acetaminophen (AC; "pharmaceuticals").

3.2.1. AC photodegradation

Degradation of a 0.16 mM (24.2 ppm) AC solution without catalyst or with TiO_2 at 0.02 g l^{-1} is shown in Fig. 3. The experiment was performed with air bubbling in the device through the auxiliary inlet (see Fig. 1) to ensure enough oxygen for the oxidative process. The figure presents linearized plots to visually evaluate the fit to zero-, first- and second-order processes (for detailed equations see Appendix 1). Non-catalyzed processes exhibited good fit to the zero-order process. A similar fit could also be seen to the second-order process, and an even slightly better fit was seen to the first-order process (Fig. 3(b) and (c)). However, differences were very small, and

Table 1
Preliminary photodegradation after 2 h in batch experiments. Catalysts, when present, were at a concentration of 0.2 g l^{-1}

Pollutant	Catalyst	Catalyzed photodegradation (%)	Photodegradation without catalyst (%)
Dyes			
Acid yellow	TiO_2	74	67
Fast green	SHCa-1	96	30
	TiO_2	97	
Fluorescein	SHCa-1	76	73
Ponceau red	SHCa-1	45	24
Rhodamine B	SHCa-1	93	77
Crystal violet	TiO_2	80	62
Acriflavine	TiO_2	98	95
Phenols			
Caffeine	TiO_2	93	19
Picric acid	TiO_2	98	10
Trichlorophenol (TCP)	SHCa-1	95	50
	Li-hectorite	94	
	SWy-2	93	
	TiO_2	96	
Pharmaceuticals			
Acetaminophen	TiO_2	99	42
Chloramphenicol	TiO_2	72	48
Tetracycline	Cu SWy-2	94	70

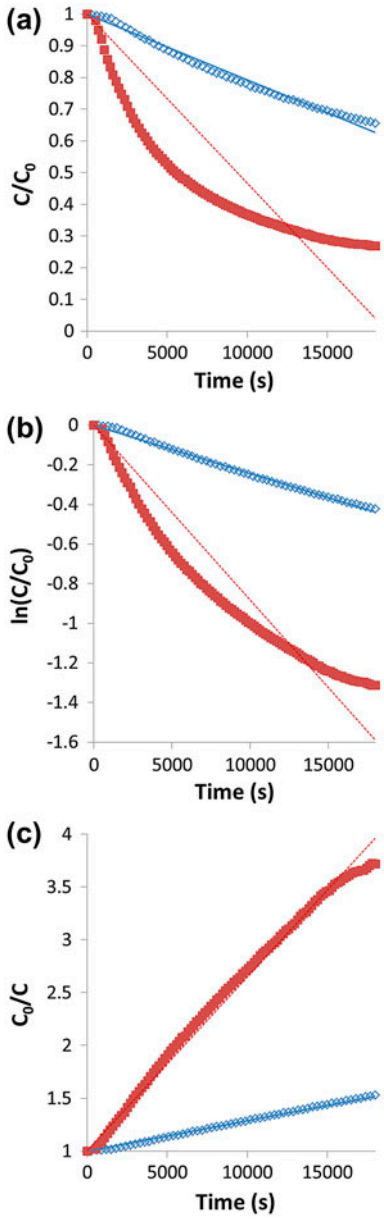

Fig. 3. Photodegradation of acetamoniphen without (clear rhombus) or with (full squares) TiO_2 as catalyst. Linearized plots are presented to visually evaluate fit to zero-order (a), first-order (b) or second-order (c) processes. The points represent measured values, while lines exhibit the fit to linearized models.

according to Occam's razor, "when you have two competing theories that make exactly the same predictions, the simpler one is the better" [27]. Thus, the zero-order fit, where the kinetic rate is independent of pollutant concentration, should be preferred for the non-catalyzed process. The decision to use zero order for the non-catalyzed process is reinforced by previous studies [28], and by the behavior of other pollutants in this study: in all cases tested, the non-catalyzed reaction could be described accurately by a zero-order process.

For the catalyzed process, a very good fit could be observed using the linearized second-order kinetics, indicating that the kinetic rate is proportional to the concentration of the pollutant squared $\left(\mathrm{d}[A]/\mathrm{d}t = -k[A]^2\right)$. The kinetics coefficients were evaluated by curve fitting using the "Solver" add-in of Excel® software, by minimizing the root mean square error (RMSE) between measured values and those calculated using Eqs. (2), (3) and 5 in Appendix 1. All parameters are presented in Table 2. The half life of the relative concentration ($t_{1/2}$) for the non-catalyzed process, assuming it indeed follows zero-order kinetics, was 24,070 s. Addition of catalyst lowered $t_{1/2}$ (assuming the process follows second-order kinetics) to 5,920 s, less than 25% of the non-catalyzed value.

Two additional experiments were performed to test additional parameters of the device: (1) the same experiment was repeated, but without bubbling of air into the reaction chamber, (2) the same experiment was repeated using SHCa-1 hectorite as the catalyst instead of TiO_2 (Fig. 4). The lack of air led to very interesting results: whereas at the beginning of the process, behavior was similar to that with added air, after approximately 10,000 s, process behavior and kinetics pattern changed completely, from a second-order to zero-order process. Measurements confirmed that dissolved oxygen decreases with time and at this stage (after about 10,000 s), the condition in the effluent was anoxic. This proves that oxygen is crucial for an efficient photocatalytic degradation of AC. Similar results for the influence of oxygen on the photodegradation of AC were reported by Moctezuma et al. [29]. However, in that study, AC was not mineralized by UVA light in the absence of catalyst. The same group also stated that the process follows first-order kinetic law [30]. In the study presented here, considerable photodegradation was achieved with UVC, even without catalyst, and the process occurred without the need for added oxygen.

SHCa-1 was tested as a catalyst since it has a surface area similar to that of P25, and in the preliminary experiments, it exhibited a catalytic efficiency similar to that of TiO_2 for some pollutants. However, this did not seem to be the case for AC: slight improvement was observed when compared to the non-catalyzed reaction, but $t_{1/2}$ only decreased to about 80% of the non-catalyzed value (19,320 s). Furthermore, the process seemed to follow a zero-order kinetics process, indicating that it occurs in a completely different path than that of the TiO_2 catalysis.

Table 2
Kinetic coefficients and curve-fitting data for the photodegradation of acetaminophen and picric acid. Half life is evaluated only for the best-fit model in each case

Pollutant	Experiment	Order	Kinetic coefficient ($\times 10^{-5}$ s^{-1})	R^2	RMSE ($\times 10^{-3}$)	$t_{1/2}$ (s)
Acetaminophen	Without catalyst	0	2.08	0.986	1.70	24070
		1	2.44	0.996	1.00	
		2	2.85	0.998	1.32	
	With TiO_2 as catalyst	0	5.33	0.827	23.01	
		1	9.93	0.954	9.74	
		2	16.90	0.994	2.91	5920
	With SHCa-1 as catalyst	0	2.58	0.995	1.60	19390
		1	3.11	0.995	2.50	
		2	2.85	0.992	6.87	
Picric acid	Without catalyst	0	4.65	0.992	3.23	10750
		1	6.00	0.995	4.37	
		2	7.61	0.983	7.83	
	With TiO_2 as catalyst	0	8.53	0.809	65.67	
		1	17.40	0.954	29.51	
		2	31.70	0.996	6.44	3150

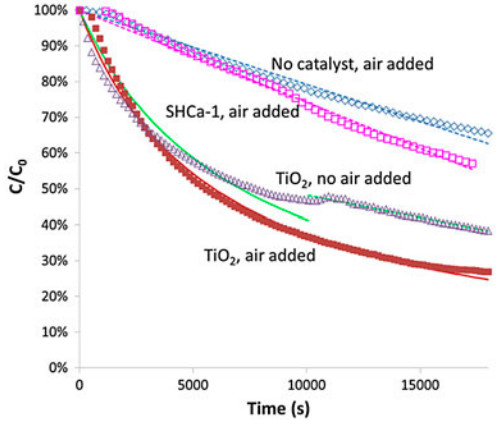

Fig. 4. Photodegradation of acetamoniphen without catalyst (clear rhombus), with TiO_2 (full squares), with SHCa-1 hectorite (clear squares), or TiO_2 without added air (clear triangles). Points present measured values, while lines exhibit the fit to linearized models.

3.2.2. PA photodegradation

Degradation of a 0.113 mM (25.8 ppm) PA solution without catalyst or with 0.02 g l^{-1} TiO_2 is shown in Fig. 5. Experiments were performed with air bubbling in the device through the auxiliary inlet (see Fig. 1). Lines represent the calculated concentrations according to zero-, first- or second-order processes (for detailed equations see Appendix 1). Parameters for the calculation were found as described for AC in Section 3.2.1. The non-catalyzed process exhibited a good fit to the zero-order process, with $t_{1/2}$ = 10,750 s. The catalyzed reaction exhibited a very good fit to a second-order process, with more than 70% reduction in half-life ($t_{1/2}$ = 3,150 s).

3.3. Confirmation experiments

To ensure that the UV–vis measurements were giving an accurate indication of the chemicals' degradation, additional experiments were performed and

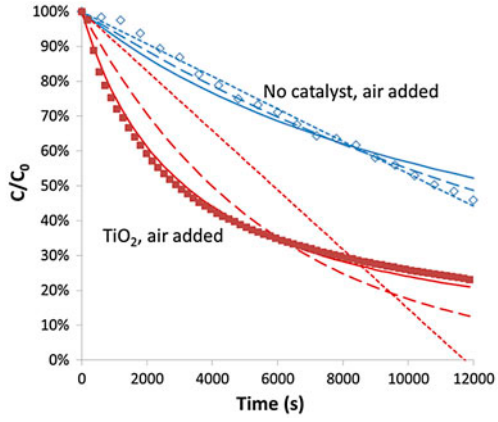

Fig. 5. Photodegradation of picric acid without (clear rhombus) or with (full squares) TiO_2 as catalyst. The points present measured values, while lines exhibit the fit to zero-order (dotted line), first-order (dashed line) or second-order (full line) process models, with the kinetic coefficients presented in Table 2.

concentration was measured at several time points by LCMS. Fig. 6 shows the degradation of PA and AC as a function of time, as measured by LCMS. The initial concentration of PA was 0.5 mM (114.5 ppm), and for AC it was 0.23 mM (33.3 ppm). In both experiments, a concentration of 0.1 ppm TiO_2 was used as the catalyst. Degradation occurred with $t_{1/2}$ values of 4,950 and 2,850 s for PA and AC, respectively. These values differed from those presented in Table 2, but this can be attributed to the different catalyst and pollutant concentrations. Experiments performed on the photodegradation of carbamazepine (Klein and Rytwo, 2013, *unpublished results)* showed that there is an optimum value for the catalyst concentration: whereas at very low values there are not enough particles to ensure efficient contact, at higher values, catalytic efficiency decreases considerably. This effect might be ascribed to TiO_2 particle aggregation [3] or high turbidity of the suspension which does not allow photons to efficiently reach the whole volume of the slurry.

In both PA- and AC-degradation experiments, intermediate compounds were screened in the middle and at the end of the experiment for m/z peaks smaller than the molecular weight of the pollutant. During PA degradation, there was no significant accumulation of any compound. However, in the case of AC, small peaks indicating the presence of butyric acid, diethylene glycol and dicyclopentadiene were measured after 130 min. In the last sample (after 300 min), the only degradation product remaining was dicyclopentadiene. Additional experiments are needed to elucidate the exact degradation pathway. A previous study [29] of AC photodegradation noted the formation of several aromatic compounds (hydroquinone, benzoquinone, p-aminophenol, p-nitrophenol) as intermediate products. However, in that case, irradiation at 365 nm (UVA) and a 2 g l^{-1} TiO_2 were used, whereas in the present study, irradiation was at 254 nm (UVC) and the catalyst concentration was 20-fold less. Indeed, even though [29] achieved complete degradation, their results seem to follow a zero-order process, i.e. there was a linear concentration decrease with time. In this study, a second-order process was observed, indicating completely different reaction paths. We assume that the large difference in the process was due to the use of UVC instead of UVA light. It is speculated that the different energies of the delivered photons lead to other degradation paths.

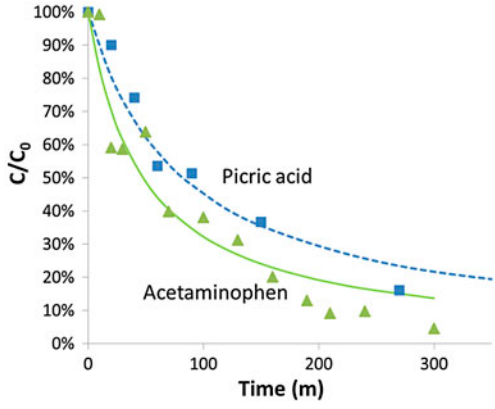

Fig. 6. Degradation of picric acid and acetaminophen as a function of time, as measured by LCMS. TiO_2 concentration: 0.1 g l^{-1}.

3.4. Open-system experiments

In all of the experiments up to this point, the initial pollutant concentrations were relatively high, enabling easy and accurate online monitoring by UV–vis spectroscopy, which is a relatively insensitive measurement technique for these pollutants. The "open system" experiments were performed with lower

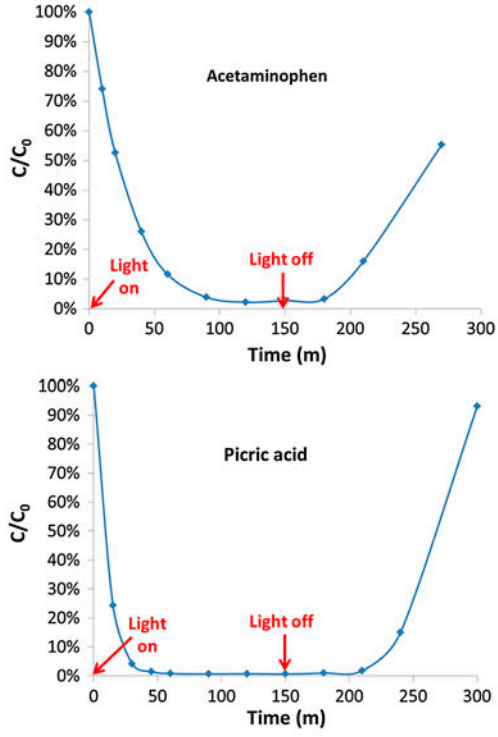

Fig. 7. Concentration of pollutants in the outflow effluent as a function of time. Initial concentration was 2 mg l^{-1}, and catalyst (TiO_2) concentration was 0.1 g l^{-1}. Flow rate of the polluted effluent was 18 ml min^{-1}, equivalent to an irradiation time of approximately 1.2 h.

initial pollutant concentrations, and measurements were performed by LCMS. Large volumes of 2 ppm pollutant solutions were prepared, and the device was filled with the solution, along with 0.1 g l^{-1} P25 TiO_2. An additional 3 l of effluent was connected to the inflow inlet of the device. The flow and lamp were switched on at the same time, and therefore the first measurement was performed on a solution that was not irradiated. As the experiment progressed, irradiation time increased up to the maximum value (1.2 h), which depends on the size of the reaction chamber and the flow rate. After 2.5 h (150 min) the lamp was shut off, but the pump continued working. Fig. 7 shows the concentration of the pollutants in the outflow effluent. The following steps could be clearly observed in the results for both PA and AC:

(1) At $t = 0$, the initial concentration was measured, since the effluent had not undergone photocatalysis.
(2) The concentration decreased, as expected, as the contact time of the pollutant solution with the light and the catalyst increased.
(3) Full degradation of AC and PA was achieved after 80 and 30 min, respectively. This fits the preliminary results (Sections 3.2.1 and 3.2.2) that showed that under identical conditions, $t_{1/2}$ of PA is lower than that of AC.
(4) After 150 min, when the lamp was shut off, the concentration started to rise. Eventually, if the experiment is long enough, the concentration should return to the initial value.

The experiment demonstrated that the photocatalytic process in the presented device may completely remove low concentrations of PA and AC.

4. Conclusions

(1) The photodegradation device presented in this study efficiently degraded PA and AC. Similar results (not shown) were obtained for other compounds, including caffeine, several cationic and anionic dyes, carbamazepine and chloramphenicol.
(2) The pollutants presented in this study were photodegraded by UVC light with no catalyst, following a zero-order process, with half lives of about 6.7 and 3 h for AC and PC, respectively. Addition of P25 TiO_2 as catalyst seemed to completely change the chemical path of the process, becoming a second-order reaction with half lives decreasing by about 75%. It should be mentioned that for all pollutants tested, the non-catalyzed reaction was zero order. Addition of TiO_2 yielded a second-order reaction for the chemicals presented in this study. With some of the other chemicals (chloramphenicol, fast green), a first-order catalyzed reaction was observed.
(3) At least in the case of AC, lack of oxygen hindered the photochemical process, changing the mechanism completely.
(4) Other catalysts can be used in the device; however hectorite clay was considerably less effective than TiO_2 in the photocatalytic degradation of AC.
(5) Additional studies are required to elucidate the exact path followed by the photodegradation process for each individual pollutant.

Acknowledgments

This study was supported by the Israeli Ministry of Economy "Kamin" 47288 project. G. Rytwo wants to thank Mr Yftah Sadan for believing, supporting, and commenting along the project. We also thank Mrs Camille Vainstein for professional English editing of the manuscript, and participants of HINT (Rational Design of Hybrid Interfaces) European COST program, Action No MP1202, for the fruitful discussions on Materials and Nanosciences.

Abbreviations

AC	—	acetaminophen (paracetamol): *N*-(4-hydroxyphenyl)ethanamide
AOP	—	advanced oxidation process
C/C_0	—	ratio of actual to initial concentration
LCMS	—	liquid chromatography mass spectrometry
LOD	—	limit of detection
OD	—	optical density
P25	—	Degussa P25 TiO_2
PA	—	picric acid: 2,4,6-trinitrophenol
RMSE	—	root mean square error
SHCa-1	—	California hectorite clay mineral
$t_{1/2}$	—	half life of relative concentration
UVC	—	100–280 nm electromagnetic radiation (light)

References

[1] H.Y. He, Photo-catalytic degradation of methyl orange in water on CuS–Cu_2S powders, Int. J. Environ. Res. 2 (2008) 23–26.
[2] A.K. Boal, C. Rhodes, S. Garcia, Pump and treat groundwater remediation using chlorine/ultraviolet advanced oxidation processes, Groundwater Monit. Rem. 35 (2015) 93–100.

[3] M.N. Chong, B. Jin, C.W.K. Chow, C. Saint, Recent developments in photocatalytic water treatment technology: A review, Water Res. 44 (2010) 2997–3027.
[4] Y. Fan, W. Ma, D. Han, S. Gan, X. Dong, L. Niu, Convenient recycling of 3D AgX/graphene aerogels (X = Br, Cl) for efficient photocatalytic degradation of water pollutants, Adv. Mater. 27 (2015) 3767–3773.
[5] J. Schneider, M. Matsuoka, M. Takeuchi, J. Zhang, Y. Horiuchi, M. Anpo, D.W. Bahnemann, Understanding TiO_2 photocatalysis: Mechanisms and materials, Chem. Rev. 114(19) (2014) 9919–9986.
[6] C.S. Uyguner, M. Bekbolet, Application of photocatalysis for the removal of natural organic matter in simulated surface and ground waters, (n.d.). Available from: <http://www.ingentaconnect.com/content/stn/jaots/2009/00000012/00000001/art00011> (accessed July 17, 2015).
[7] M.J. Benotti, B.D. Stanford, E.C. Wert, S.A. Snyder, Evaluation of a photocatalytic reactor membrane pilot system for the removal of pharmaceuticals and endocrine disrupting compounds from water, Water Res. 43 (2009) 1513–1522.
[8] T. Ohno, K. Sarukawa, K. Tokieda, M. Matsumura, Morphology of a TiO_2 photocatalyst (Degussa, P-25) consisting of anatase and rutile crystalline phases, J. Catal. 203 (2001) 82–86.
[9] B. Ohtani, O.O. Prieto-Mahaney, D. Li, R. Abe, What is Degussa (Evonik) P25? Crystalline composition analysis, reconstruction from isolated pure particles and photocatalytic activity test, J. Photochem. Photobiol. A Chem. 216 (2010) 179–182.
[10] J.H. Ramirez, C.A. Costa, L.M. Madeira, G. Mata, M.A. Vicente, M.L. Rojas-Cervantes, A.J. López-Peinado, R.M. Martín-Aranda, Fenton-like oxidation of Orange II solutions using heterogeneous catalysts based on saponite clay, Appl. Catal. B Environ. 71 (2007) 44–56.
[11] M.Y. Ahn, T.R. Filley, C.T. Jafvert, Photodegradation of decabromodiphenyl ether adsorbed onto clay minerals, metal oxides, and sediment, Environ. Sci. Technol. 40 (2006) 215–220.
[12] B. Iurascu, I. Siminiceanu, D. Vione, M.A. Vicente, A. Gil, Phenol degradation in water through a heterogeneous photo-Fenton process catalyzed by Fe-treated laponite, Water Res. 43 (2009) 1313–1322.
[13] J.J. Werner, K. McNeill, W.A. Arnold, Photolysis of chlortetracycline on a clay surface, J. Agric. Food Chem. 57 (2009) 6932–6937.
[14] S. Xu, H. Lu, L. Chen, X. Wang, Molecularly imprinted TiO_2 hybridized magnetic Fe_3O_4 nanoparticles for selective photocatalytic degradation and removal of estrone, RSC Adv. 4 (2014) 45266–45274.
[15] G. Centi, S. Perathoner, T. Torre, M.G. Verduna, Catalytic wet oxidation with H_2O_2 of carboxylic acids on homogeneous and heterogeneous Fenton-type catalysts, Catal. Today 55 (2000) 61–69.
[16] J. Herney-Ramirez, M.A. Vicente, L.M. Madeira, Heterogeneous photo-Fenton oxidation with pillared clay-based catalysts for wastewater treatment: A review, Appl. Catal. B Environ. 98 (2010) 10–26.
[17] D. Chen, G. Du, Q. Zhu, F. Zhou, Synthesis and characterization of TiO_2 pillared montmorillonites: Application for methylene blue degradation, J. Colloid Interface Sci. 409 (2013) 151–157.
[18] H. Bel Hadjltaief, M.E. Galvez, M. Ben Zina, P. Da Costa, TiO_2/clay as a heterogeneous catalyst in photocatalytic/photochemical oxidation of anionic reactive blue 19, Arab. J. Chem. (2014).
[19] L.Y. Zou, Y. Li, Y.-T. Hung, Wet air oxidation for waste treatment, Adv. Physicochem. Treat. Technol. 5 (2007) 575–610.
[20] J.-M. Herrmann, Heterogeneous photocatalysis: Fundamentals and applications to the removal of various types of aqueous pollutants, Catal. Today 53 (1999) 115–129.
[21] R.L. Pozzo, J.L. Giombi, M.A. Baltanás, A.E. Cassano, The performance in a fluidized bed reactor of photocatalysts immobilized onto inert supports, Catal. Today 62 (2000) 175–187.
[22] M. Rivero, S. Parsons, P. Jeffrey, M. Pidou, B. Jefferson, Membrane chemical reactor (MCR) combining photocatalysis and microfiltration for grey water treatment, Water Sci. Technol. 53 (2006) 173–180.
[23] Y. Meng, X. Huang, Q. Yang, Y. Qian, N. Kubota, S. Fukunaga, Treatment of polluted river water with a photocatalytic slurry reactor using low-pressure mercury lamps coupled with a membrane, Desalination 181 (2005) 121–133.
[24] S. Mozia, M. Tomaszewska, A.W. Morawski, A new photocatalytic membrane reactor (PMR) for removal of azo-dye Acid Red 18 from water, Appl. Catal. B Environ. 59 (2005) 131–137.
[25] S. Mozia, M. Tomaszewska, A.W. Morawski, Photocatalytic membrane reactor (PMR) coupling photocatalysis and membrane distillation—Effectiveness of removal of three azo dyes from water, Sel. Contrib. 4th Eur. Meet. Sol. Chem. Photocatal. Environ. Appl. (SPEA 4) 129 (2007) 3–8.
[26] G. Rytwo, G. Daskal, A system for treatment of polluted effluents by photocatalysis, Intellect. Prop. Off. Newport, UK Patent Application Number 1416495.8, 2014.
[27] P. Gibbs, What is Occam's Razor? Orig. Usenet Phys. FAQ, Univ. California, Riverside, 1996. Available from: <http://math.ucr.edu/home/baez/physics/General/occam.html> (accessed December 21, 2014).
[28] M. Samuels, O. Mor, G. Rytwo, Metachromasy as an indicator of photostabilization of methylene blue adsorbed to clays and minerals, J. Photochem. Photobiol. B Biol. 121 (2013) 23–26.
[29] E. Moctezuma, E. Leyva, C.A. Aguilar, R.A. Luna, C. Montalvo, Photocatalytic degradation of paracetamol: Intermediates and total reaction mechanism, J. Hazard. Mater. 243 (2012) 130–138.
[30] C. Aguilar, C. Montalvo, J.G. Ceron, E. Moctezuma, Photocatalytic degradation of acetaminophen, Int. J. Environ. Res. 5 (2011) 1071–1078. Available from: <http://www.ijer.ir/?_action=articleInfo&article=465&vol=21> (accessed December 24, 2014).
[31] D.P. White, Chapter 14-Chemical Kinetics, Cent. Sci., nineth ed., Prentice-Hall, 2003. Available from: <my.ilstu.edu/~ccmclau/che141/materials/outlines/chapter14.ppt>.
[32] G. Rytwo, Y. Gonen, Functionalized activated carbons for the removal of inorganic pollutants, Desalin. Water Treat. 11 (2009) 318–323.

Appendix 1. Kinetic models

The order of the process is defined by its fit to the equation:

$$v = \frac{\mathrm{d}[C]}{\mathrm{d}t} = k[C]^{\mathrm{a}} \tag{1}$$

where v is the reaction rate (the rate at which the concentration C of the pollutant changes with time), k is the kinetics coefficient, and a is the order of the process—which is found empirically and is related to the mechanism by which the process occurs [31].

To simplify the calculations, avoid unit mismatches, and allow comparison between parameters in different reaction mechanisms, A, the "relative concentration at time t" is defined as C_t/C_0 (the ratio of actual to initial concentration); thus $A_0 = 1$. Since A is dimensionless, none of the parameters have concentration units. This is convenient, since it yields kinetic coefficients that always have dimensions per time, regardless of the order of the process.

A zero-order process is one in which $\mathrm{d}[A]/\mathrm{d}t = -k[A]^0 = -k$. Thus, in a zero-order process, the reaction rate is not a function of the reactant concentration. Integration of this equation gives:

$$[A] = [A]_0 - kt = 1 - kt \tag{2}$$

Thus, a linear representation of $[A]$ as a function of time will yield the fit to a zero-order process, and the slope will be the kinetic coefficient. The half life can be calculated as $t_{1/2} = 1/2k$. It should be noted that without transforming to relative concentrations (C/C_0), $t_{1/2}$ would depend on the initial concentration.

A first-order reaction means that the reaction proceeds at a rate that depends linearly on the concentration of the reactant (this means that the rate at which a reactant is consumed is proportional to its concentration at that time). A first-order process is one in which $\mathrm{d}[A]/\mathrm{d}t = -k[A]^1 = -k[A]$.

Integration of this equation leads to:

$$[A] = \frac{[C]}{[C]_0} = e^{-kt} \tag{3}$$

which can be linearized to $\ln[A] = -kt$. Thus, a linear representation of the logarithm of $[A]$ as a function of time will yield the fit to a first-order process, and the slope will be the kinetic coefficient. The half life can be calculated as:

$$t_{1/2} = \frac{-\ln(1/2)}{k} = \frac{\ln 2}{k} \tag{4}$$

and is independent of the initial concentration, even without transformation to relative concentration [32].

A second-order process is one in which $\mathrm{d}[A]/\mathrm{d}t = -k[A]^2$. This means that the reaction proceeds at a rate that depends on the concentration of the reactant squared (i.e. the rate at which a reactant is consumed is proportional to its concentration to the second power at that time). Integration of this equation leads to:

$$\frac{1}{[A]} = kt + 1 \tag{5}$$

Thus, a linear representation of the reciprocal of $[A]$ as a function of the time will yield the fit to a second-order process, and the slope will be the kinetic coefficient. The half life is calculated by $t_{1/2} = 1/k$. As in the zero-order case, without transforming it to relative concentration, $t_{1/2}$ would depend on the initial concentration.

The equations presented here are generally referred to as "pseudo-order equations", since they consider only the concentration of one component (in this case, the pollutant). This assumption is logical when either the other components (in this case, photons, catalyst, auxiliary compounds such as O_2, etc.) do not influence the process ("are of zero order"), or their concentration is so large that no measurable changes can be observed. In our case, we also assume that the products do not influence the photodegradation process, and therefore the "backward" reaction has a very low kinetic coefficient.